

## Fabrication of silicon carbide particles from recycled polysilicon photovoltaic cells

Ah Hyun Oh<sup>a,†</sup>, Hyeon Seung Lee<sup>a,†</sup>, Bong-Gu Kim<sup>b</sup>, Sung-Churl Choi<sup>a</sup>, Yeon-Gil Jung<sup>b</sup> and Gye Seok An<sup>a,\*</sup>

<sup>a</sup>Division of Materials Science and Engineering, Hanyang University, 222 Wangsimni-ro, Seongdong-gu, Seoul 04763, Republic of Korea

<sup>b</sup>School of Materials Science and Engineering, Changwon National University, 20 Changwondaehak-ro, Changwon, Gyeongnam, 51140, Republic of Korea

In this study, a recycling method for the recovery of polysilicon (poly-Si) wafers from end-of-life poly-Si photovoltaic (PV) cells and the synthesis of high-purity silicon carbide (SiC) using the recovered poly-Si wafers are reported. First, an end-of-life poly-Si PV module was etched by acid treatment, using a mixture of hydrofluoric acid (HF) and nitric acid (HNO<sub>3</sub>), to recover the poly-Si wafer. The purified wafer was milled using high-energy milling to form Si powders to prepare a fine SiC powder. Then, the SiC powder was synthesised using spark plasma sintering with a mixture of poly-Si powder and carbon black. By analysing the morphology and crystal structure of the SiC powders synthesised at different reaction temperatures, the optimum temperature for synthesising the fine SiC powder was determined. After milling, the poly-Si and SiC powders were washed using a HF solution to remove the oxide impurities from the powders. Thus, a fine SiC powder with an oxygen content of 0.11% was obtained.

**Key words:** Polysilicon photovoltaic cell, Recycle, High-energy milling, Silicon carbide, Spark plasma sintering.

### Introduction

Photovoltaics (PVs) have received significant attention as a renewable energy source; thus, deployment of solar modules has rapidly increased [1]. However, PV modules have a limited lifetime of 25–30 years. Hence, with the rapid deployment of PV modules, an increase in waste modules is expected [2]. Generally, the end-of-life PV modules are landfilled or incinerated, which can lead to serious environmental pollution [3,4]. To solve this problem, various recycling methods for unserviceable PV modules have been proposed.

In particular, the recycling of polysilicon (poly-Si) wafers in poly-Si PVs has been actively researched following the increase in industrial application and transition to other materials, particularly silicon carbide (SiC), which has attracted significant attention. Cubic-structured SiC is a ceramic carbide material with strong covalent bonds that possesses high mechanical strength, hardness, thermal conductivity, thermal shock resistance, good corrosion resistance, and semi-conductivity [5–7]. Therefore, it has been used in various industrial applications such as in semiconductors, heating elements, and extreme-environment materials [8]. Because SiC exhibits its superior characteristics when in the form of fine powders, the demand for fine SiC powders have

steadily increased. Therefore, fabrication of fine SiC powders using poly-Si wafers recovered from end-of-life poly-Si PV cells offers significant industrial potential.

In this study, fine SiC powder was synthesised using poly-Si wafers recovered from an end-of-life poly-Si PV cell. To obtain high-quality poly-Si wafers, the poly-Si PV cell was etched using mixed acid consisting of hydrofluoric acid (HF) and nitric acid (HNO<sub>3</sub>). The recovered poly-Si wafer was milled using a high-energy mill and washed with an HF solution to remove the oxide impurities produced during milling. In the process, the oxide-impurity removal efficiency, which depended on the HF concentration, was investigated. SiC was synthesised by making the Si powder react with carbon using spark plasma sintering (SPS), which could reduce the synthesis time and minimise particle growth [9,10]. The effect of synthesis temperature was examined by investigating the crystal phase and morphology. The synthesised SiC was washed several times using an HF solution, and the oxide-removal efficiency was investigated.

### Experimental procedure

#### Recovery of poly-Si wafer

The poly-Si wafer was recovered from a poly-Si PV cell using acid treatment. The acid treatment was performed using a mixed acid consisting of HF (49%–52%, Duksan Pure Chemicals Co. Ltd., Korea) and HNO<sub>3</sub> (60%–62%, Junsei Chemical Co., Ltd., Japan).

\*Corresponding author:  
Tel : +82-2-2220-0505  
Fax: +82-2-2291-6767  
E-mail: faustmaro@hanyang.ac.kr

<sup>†</sup>These authors contributed equally to this work.

The poly-Si PV cell (SH-1880S3N-M, 6", Shinsung Solar Energy Co., Ltd., Korea) was immersed into 1 L of the mixed acid, which was prepared by mixing HF, HNO<sub>3</sub>, and water in a volume ratio of 5:30:65 and etched for 15 min at 80 °C on a hot plate. Then, the etched cell was washed several times and dried at 60 °C for 1 h in a vacuum drying oven.

### Grinding and washing of poly-Si wafer

The recovered poly-Si wafer was initially crushed using a zirconia mortar for 2 h. Subsequently, it was put into a SiC jar (48 × 51 mm, laboratory grade) with a SiC ball (10 mm in diameter) whose weight depended on the ball-to-powder ratio (BPR) of 2.55:1. Thereafter, the Si powder was pulverised in a SPEX mill (8000D, SPEX SamplePrep, USA), which can provide high impact energy to the powder by increasing the milling time from 2 to 20 h. After milling, the 0.5 g of Si powder was washed with 40 mL of 1 wt%–5 wt% HF solution and water several times. Then, the powder was dried at 70 °C for 6 h under a vacuum pressure of  $1 \times 10^{-2}$  Torr in a vacuum drying oven.

### Synthesis of SiC powder

To synthesise SiC, the as-prepared Si powder and carbon black (99.9%, Alfa Aesar, USA) were used as the initial materials for Si and C, respectively. Si and the carbon black powder were mixed at a 1:1.8 molar ratio using a ball mill for 48 h at 200 rpm in a polypropylene bottle with SiC balls (10 mm in diameter) with an adjusted BPR of 10:1. The mixed powder was pressed by 12.5-MPa pressure in a graphite die (inner diameter: 12.7 mm). The graphite die was installed in the SPS furnace (EL tek Korea, Korea) and treated under 30 MPa pressure in vacuum at the temperature range of 1200–1400 °C (heating rate: 100 °C/min) for 1 h. The synthesised SiC was crushed by the SPEX mill for 2 h using a 10-mm-diameter SiC ball and pulverised by a sieving process. Then, 0.5 g of SiC powder was washed several times with 40 mL of 5 wt% HF solution and water and subsequently dried at 70 °C for 6 h in a vacuum dryer under  $1 \times 10^{-2}$  Torr of

vacuum pressure in a vacuum drying oven.

### Characterisation

The morphologies and compositions of the wafer and particles were analysed using field emission scanning electron microscopy [(FE-SEM), JSM-6330F, JEOL, Japan] and energy-dispersive spectroscopy [(EDS), EDAX detector (DPP-II), USA], respectively. The elemental composition of the recovered Si wafer was quantitatively analysed using glow-discharge mass spectrometry [(GDMS), GD90RF, Msi, UK]. The particle size of the milled Si powder was measured using the dynamic light scattering (DLS) method (Zetasizer Nano ZS, Malvern, USA). The changes in the oxygen contents that remained in the Si and SiC powder were measured using a nitrogen/oxygen determinator (TC-600, LECO Co., USA). The crystal structure of the synthesised SiC particle was analysed by X-ray diffraction [(XRD), Ultima IV, Rigaku, Japan] with Cu-K $\alpha$  radiation ( $\lambda = 1.5418 \text{ \AA}$ ).

### Results and Discussion

The photographic images of the front and back sides of the poly-Si PV cell before and after etching are shown in Fig. 1. Before etching, the front side showed the deposition of a blue SiN<sub>x</sub> anti-refracting coating layer and Ag electrode. After etching by the acid treatment, the Ag electrode was removed from the surface of the PV cell; however, an indentation remained in its place. Similarly, the SiN<sub>x</sub> anti-refracting coating layer was removed, leaving a stripe mark at its original position. Additionally, some random scratches were observed at the front side of the etched PV cell, which were presumed to occur due to the friction between the PV cell and tray during the etching process. On the other hand, the back side of the PV cell exhibited a white line corresponding to the Ag/Al soldering pad and Al-back surface field. Similar to the case at the front side, the Ag/Al soldering pad on the back side disappeared after the acid treatment, leaving behind an indentation. In addition, the Al-back surface field was

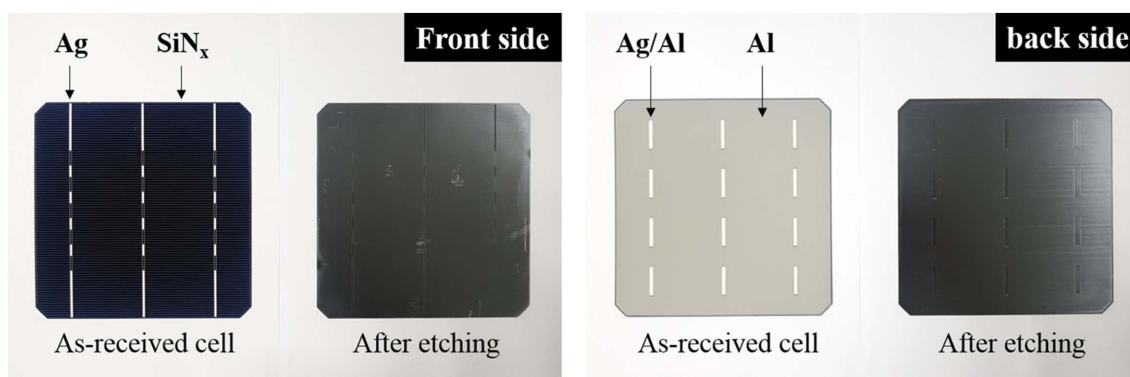
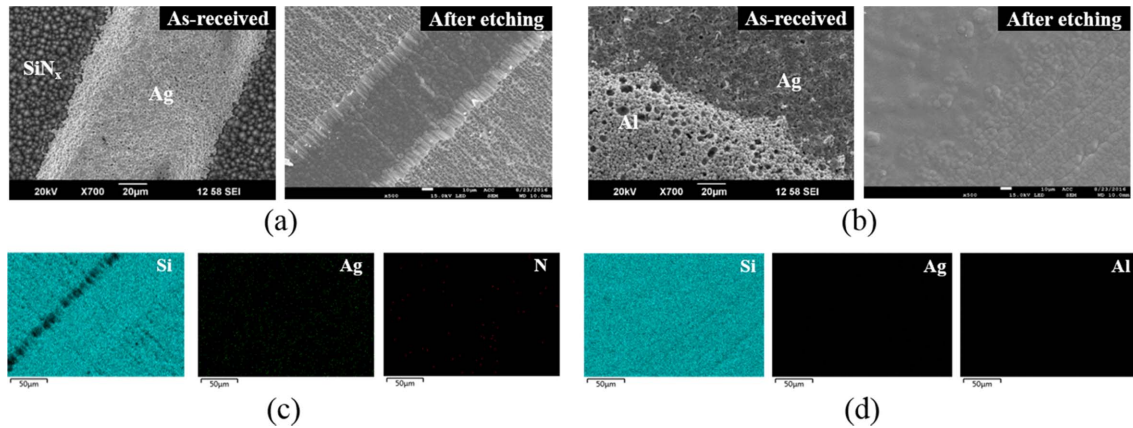


Fig. 1. Photographic images of the front and back sides of the poly-Si PV cell before and after etching.



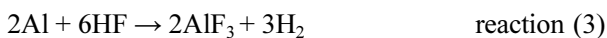
**Fig. 2.** SEM images of (a) front and (b) back sides of the PV cell with and without etching and EDS mapping results of etched (c) front and (d) back sides.

removed, and line marks, which were assumed to be generated during the production of poly-Si wafer, were left in the back field. Overall, Ag, Al, and  $\text{SiN}_x$  appeared to have been eliminated from the front and back sides of the etched PV cell, and only the poly-Si remained.

SEM was performed to observe the changes in the morphology before and after etching, and EDS was simultaneously performed for qualitative analysis of the etched PV cell (Fig. 2). Before etching, the front side of the as-received PV cell showed aggregated  $\text{SiN}_x$  and Ag particles along the  $\text{SiN}_x$  anti-reflecting coating layer and Ag electrode area, respectively [Fig. 2(a)]. After the etching, the aggregated particles disappeared, and an indentation was left in place of the Ag electrode. After the etching, the aggregated particles disappeared, and an indentation was left in place of the Ag electrode.  $\text{SiN}_x$  and Ag reacted with HF and  $\text{HNO}_3$  in the acid solution as follows:



According to reactions (1) and (2),  $\text{SiN}_x$  and Ag were detached from the front of the PV cell due to vaporisation or dissolution into the solution in an ionised state. Similarly, the back [Fig. 2(b)] exhibited aggregated Ag and Al particles along the Ag/Al soldering pad and Al back-surface-field area, respectively, before etching. After the etching, the area comprising the aggregated particles was eliminated, and slight line marks were left in place of Al. The Ag, which was deposited as a soldering material, reacted with the acid solution according to reaction (1), whereas the Al in the back-surface field reacted according to reaction (3).



Because of these reactions, Ag and Al could be separated in the gas or ionised state in the acid solution. The removal of the deposited materials by the

**Table 1.** Contents of the main elements of etched poly-Si PV cells as determined by GDMS

Element	Elemental composition (ppm)
Silicon (Si)	999,985.94
Silver (Ag)	<0.001
Aluminum (Al)	<0.001

acid treatment was confirmed from the EDS mapping results. The EDS data indicated the removal of the Ag electrode and  $\text{SiN}_x$  coating layer from the front side [Fig. 2(c)] and Ag/Al soldering pad and Al back surface field from the back side [Fig. 2(d)], which exposed the Si wafer.

The elemental composition of the etched poly-Si PV cell was analysed using GDMS, and a summary of the contents of the main elements is listed in Table 1. After the etching, the Si content was 999985.94 ppm (99.998594%), which implied high purity. On the other hand, the Ag and Al contents, which were deposited as the electrode and back-field layer, respectively, were below 0.001 ppm (0.0000001%), which was beyond the measurable range of the GDMS. These results suggested that the poly-Si wafer recovered from the poly-Si PV cell was highly pure and almost free of impurities; hence, the recovered poly-Si could be used as a starting material for high-purity SiC.

Fig. 3 shows the SEM images of the poly-Si wafer obtained by varying the milling time. The initial hand-ground Si wafer [Fig. 3(a)] contained a layered and microsized plate structure. The plate structure, which had the characteristic of poly-Si wafers, could not be transformed into other shapes by hand grinding using a mortar. When the Si wafer was milled for 2 h using the SPEX mill, a small amount of the plate structure remained, and the milled particles aggregated [Fig. 3(b)]. After 4 h of milling, the plate structure of the Si wafer almost disappeared [Fig. 3(c)]. The transformation of the individual particles started after 6 h of

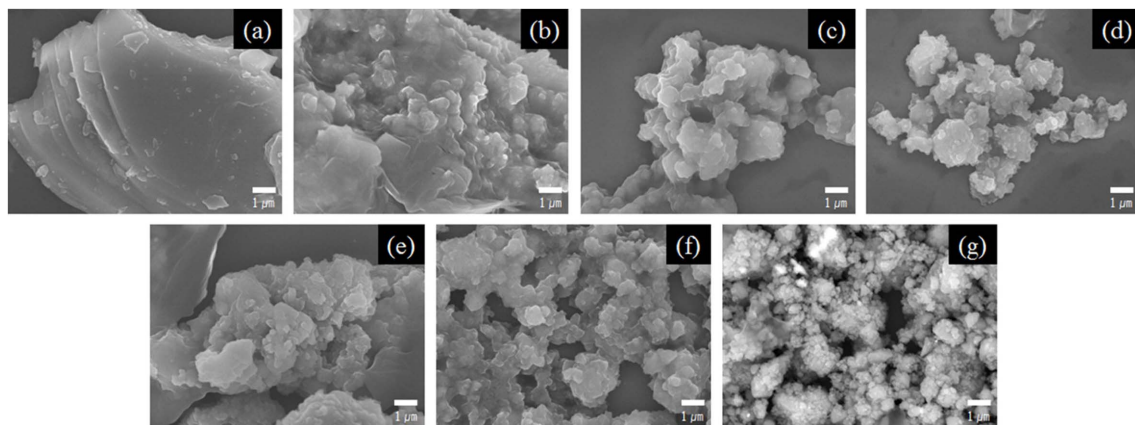


**Fig. 3.** SEM images of the poly-Si wafer showing variations in the morphology with milling time. (a) Initial hand-ground Si wafer at (b) 2 h, (c) 4 h, (d) 6 h, (e) 8 h, (f) 10 h, and (g) 20 h.

milling. Beyond this time, the particle size of the Si powder steadily decreased with the increase in the milling time [Fig. 3(d)]. The particle size continued to decrease and was finally reduced to the nanoscale size after 20 h of milling [Fig. 3(g)].

Meanwhile, some impurities appeared in the poly-Si particles milled using the SPEX mill. To identify the impurities, the surface functional groups of the Si wafer, which were hand-ground and SPEX-milled for 10 h, were investigated using Fourier transform infrared (FT-IR) spectroscopy (Fig. 4). The O–H stretching and bending vibration peaks were observed at approximately  $3,074\text{--}3,749\text{ cm}^{-1}$  and  $1,631\text{ cm}^{-1}$ , respectively, because of the presence of the hydroxyl group (Si–OH) in all samples [11–13]. Additionally, siloxane (Si–O–Si) and silanol (Si–OH) functional groups appeared at  $1,192$  and  $1,049\text{ cm}^{-1}$ , respectively [14, 15]. The absorption peak intensities of the SPEX-milled Si wafer over the entire wavenumber range were much higher than those of the Si wafer before milling, which indicated that the oxidation of Si occurred even before milling. However, the oxidation significantly progressed after milling. As a result, SiO<sub>2</sub> was formed on the Si powder because SiO<sub>2</sub> was dominantly generated from the Si oxidation.

The average particle size of the poly-Si wafer investigated using the DLS method with varying milling time is shown in Fig. 5. Each sample was measured five times. As shown, the particle size decreased with the increase in the milling time. After 2 h of milling, the average particle size of poly-Si was  $1.14\text{ }\mu\text{m}$  and decreased to  $790\text{ nm}$  at 4 h of milling. The average particle size steadily decreased to  $512$ ,  $398$ , and  $311\text{ nm}$  after 6, 8, and 10 h of milling, respectively. This tendency continued up to 20 h of milling; at this stage the average particle size was  $202\text{ nm}$ . Furthermore, the standard deviation of the particle size of the milled powder decreased from  $70$  to  $30\text{ nm}$  after 20 h of milling. Therefore, milling resulted not only in particle-size reduction, but also in particle-size homogeneity.

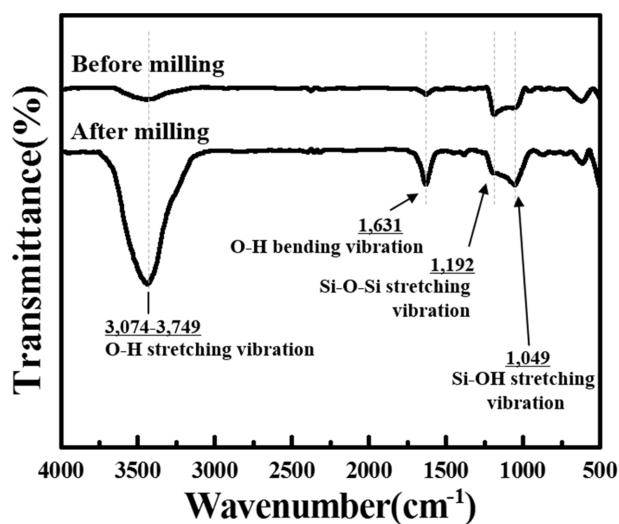


**Fig. 4.** FT-IR spectra of the hand-ground and 10 h milled poly-Si wafer.

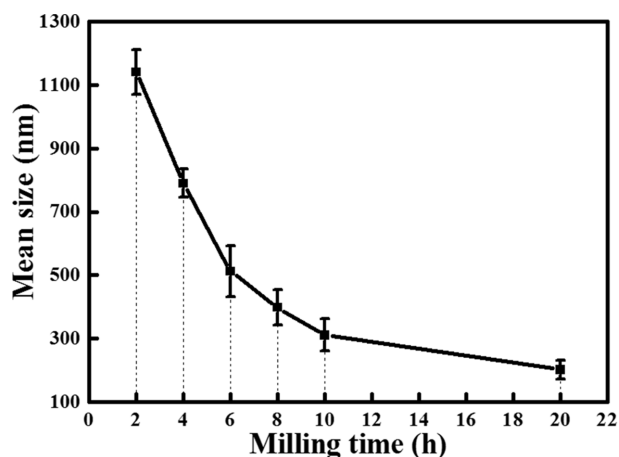
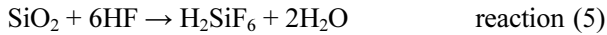


**Fig. 5.** Average particle size of the poly-Si wafer according to the milling time.

To remove the SiO<sub>2</sub> that was formed during the milling of poly-Si wafer, the Si powder was washed

with HF solution. SiO<sub>2</sub> reacted with HF as follows:



According to reactions (4) and (5), SiO<sub>2</sub> reacted with HF to produce H<sub>2</sub>O and SiF<sub>4</sub> gas or ionised H<sub>2</sub>SiF<sub>6</sub>, which could be removed from the surface of the Si particles. A dilute HF solution with a concentration in the range of 1–5 wt% was used, and washing was performed using 40 mL of HF solution per 0.5 g of milled Si powder. The oxygen content of the Si powder according to the HF concentration of the washing solution is shown in Fig. 6. The oxygen content of the poly-Si particles before washing was 1.6% and decreased to 0.4% when washed with 1 wt% HF solution. With the increase in the HF concentration from 2 wt% to 5 wt%, the oxygen content of the Si powder decreased to 0.15%, 0.05%, 0.07%, and 0.01%, respectively. Thus, the oxygen content decreased depending on the HF concentration in the washing solution. Additionally, 3 wt% HF could be considered as the optimal concentration because the oxygen content sharply dropped at 3 wt% HF, and only slight changes were observed at higher concentrations. However, because the standard deviation was 0.04% at 3 wt% and 0.026% at 5 wt%, the 5 wt% concentration with a low standard deviation was considered as the optimal HF concentration.

Table 2 lists the synthesis routes to SiC and the Gibbs free-energy change corresponding to the reactions [16, 17]. Fig. 7 shows a summary of the Gibbs free energy

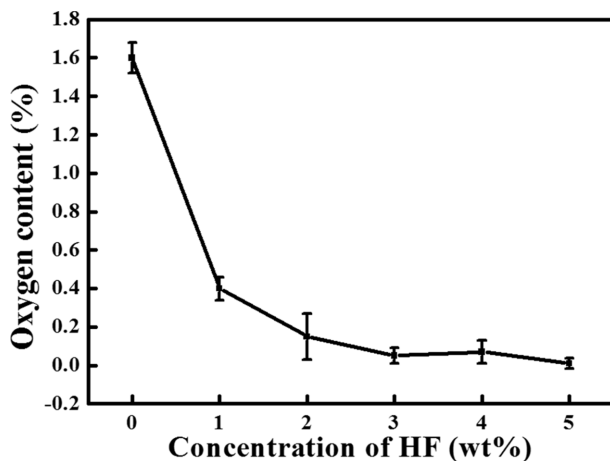


Fig. 6. Variation in the oxygen content with HF concentration.

of the reaction listed in Table 2. When SiO<sub>2</sub> was used as a Si source, SiC was synthesised by reaction (6) in which SiO<sub>2</sub> and C reacted to form SiC and gaseous CO. Because the calculated thermodynamic reaction temperature of reaction (6) was 1735 K (1462 °C), the reaction occurred at a temperature higher than 1735 K (1462 °C). Meanwhile, in the present study, the possible reactions were assumed as reactions (7) and (8) because a previously recovered Si powder was directly used. In addition, reaction (9), which combined reactions (7) and (8), was considered to be dominant during the synthesis. The change in the Gibbs free energy in reaction (9) had a negative value in the temperature range of 1400–1900 K; thus, SiC synthesis was considered possible in the temperature range of 1473–1673 K (1200–1400 °C), which was lower than that for the reaction using SiO<sub>2</sub>.

The SiC samples were synthesised by SPS using a mixture of Si and carbon black at a molar ratio of 1:1.8 in the temperature range of 1200–1400 °C. The XRD profiles of the samples are shown in Fig. 8. In the case of the samples synthesised at temperatures above 1300 °C, diffraction peaks appeared at 35.64°, 41.26°, 60.08°, 71.82°, and 74.72° corresponding to the (111), (200), (220), (311), and (222) planes of SiC, respectively (JCPDS #73-1665) [18]. On the other hand, in the samples synthesised at 1200 and 1250 °C, diffraction peaks appeared at 28.42° and 46.92° corresponding to the (111) and (220) planes of Si and SiC, respectively (JCPDS #27-1402) [19]. However, the low intensity of

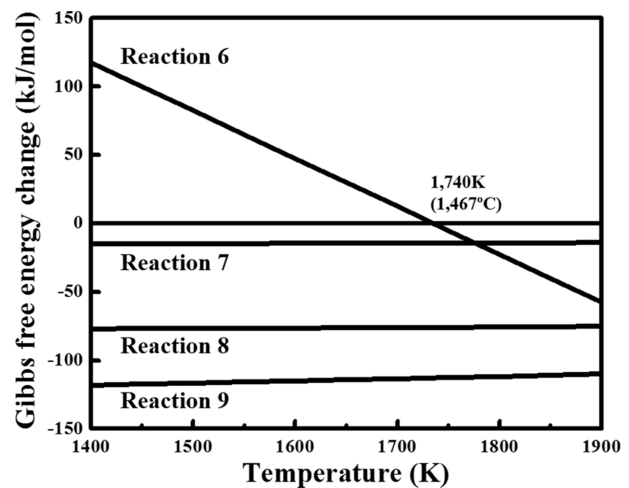
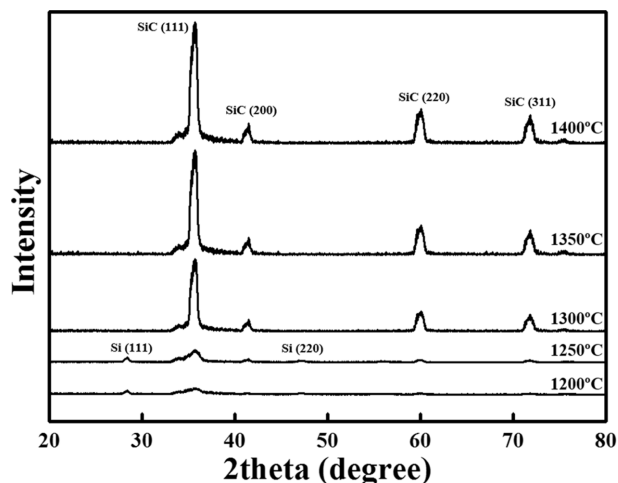


Fig. 7. Gibbs free energy as a function of temperature for the SiC generation reactions.

Table 2. Free-energy data of the Si–C, SiO–C, SiO<sub>2</sub>–C, and Si–SiO–C systems

	Chemical reaction	$\Delta G$ (kJ/mol)
Reaction (6)	$\text{SiO}_2 + 3\text{C} = \text{SiC} + 2\text{CO}(\text{g})$	$609023 - 351 \cdot T$
Reaction (7)	$\text{Si} + \text{C} = \text{SiC}$	$-17220 + 1.68 \cdot T$
Reaction (8)	$\text{SiO} + 2\text{C} = \text{SiC} + \text{CO}(\text{g})$	$-19660 - 0.9 \cdot T$
Reaction (9)	$\text{Si} + \text{SiO} + 3\text{C} = 2\text{SiC} + \text{CO}(\text{g})$	$-141500 + 16.6 \cdot T$



**Fig. 8.** XRD profiles as a function of synthesis temperature (1200–1400 °C).

Si and SiC peaks indicated a low degree of crystallisation; thus, the crystallinity was considered uncertain. These results indicated that a temperature of 1300 °C or higher is required for the synthesis of crystalline SiC [17].

Fig. 9 shows the SEM images of the SiC synthesised in the temperature range of 1300–1400 °C. Crystalline SiC was formed in all the investigated temperatures; however, the particle size gradually increased with the increase in temperature. The SiC synthesised at 1300 °C contained particles with sizes in the range of 200–300 nm [Fig. 9(a)], whereas SiC synthesised at 1350 °C had larger particles [Fig. 9(b)]. At 1400 °C, the particles grew to a size of approximately 2–3 μm [Fig. 9(c)]. Because finer particles were formed at 1300 °C compared with those formed at other temperatures, this temperature was considered as the optimal temperature for synthesising fine crystalline SiC.

The synthesised SiC was washed using an HF solution to remove the oxides in the SiC powder, and the variation in the oxygen content with the number of washing cycles is shown in Fig. 10. Because 5 wt% was found to be the optimal concentration for removing SiO<sub>2</sub>, 5 wt% HF solution was used at this stage. We used 40 mL of HF solution per 0.5 g of SiC powder. Five measurements were performed for each specimen, and the error was recorded. SiC before washing contained

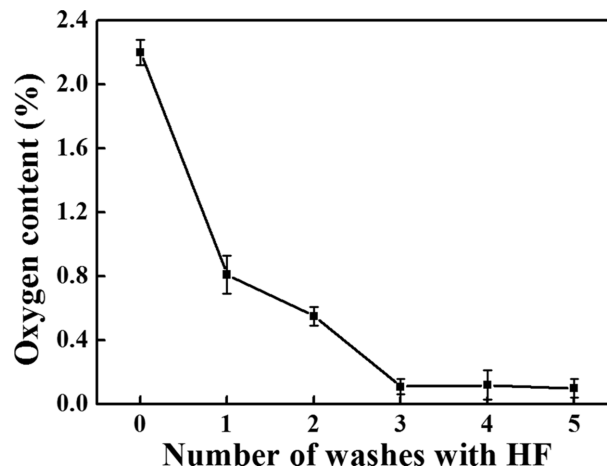


**Fig. 10.** Variation in the oxygen content of the SiC powder washed with 5 wt% HF solution according to the number of washing cycles.

approximately 2.2% oxygen, which decreased to 0.55%, 0.11%, 0.12%, and 0.1% with the increase in the number of washing cycles. Thus, the HF solution could remove the oxide impurity during the washing process, and increasing the number of washing cycles could lower the oxygen content. Further, the oxygen content rapidly decreased up to three washing cycles. Beyond this number, it remained almost constant. In addition, beyond three washing cycles, the standard deviation of the oxygen content increased from 0.05% to 0.09%. Therefore, we believed that washing once and twice could not sufficiently remove the impurities, depending on the completion of chemical reaction, and three washing cycles could most efficiently remove the oxide impurity.

## Conclusion

A poly-Si wafer was recovered from a poly-Si PV cell by acid treatment using a mixed acid composed of HNO<sub>3</sub> and HF, which resulted in the removal of deposited materials such as Ag, Al, and SiN<sub>x</sub>, leaving only the Si wafer behind. The content of the removed elements was less than 0.0000001%, whereas the residual Si content was 99.998594%. The recovered poly-Si wafer was milled for 20 h using a SPEX mill to

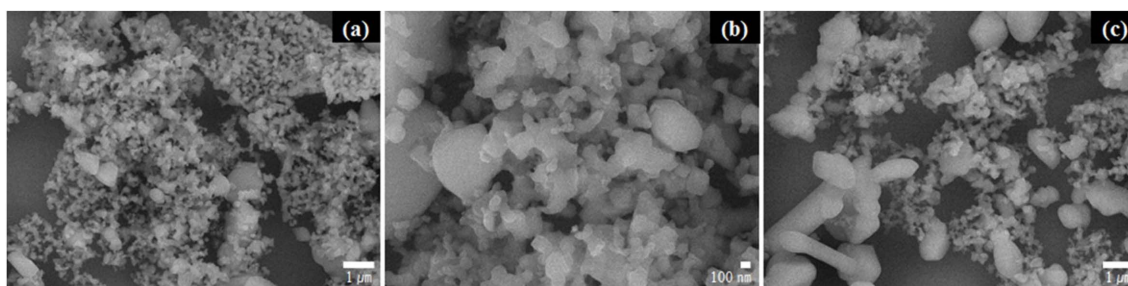


**Fig. 9.** SEM images of the SiC particles synthesised at (a) 1300 °C, (b) 1350 °C, and (c) 1400 °C.

prepare 200-nm-size particles. However, an oxide impurity ( $\text{SiO}_2$ ) was produced by the milling process. This impurity was eliminated by washing the particles with a 5 wt% HF solution, which reduced the oxygen content in the Si powder to 0.01%. The Si powder and carbon black were mixed in 1:1.8 molar ratio, and SiC was synthesised using SPS performed at a temperature in the range of 1200–1400 °C. The XRD analysis showed that the intensity of Si and SiC peaks were low, which indicated uncertain crystallinity due to low crystallisation at 1200 and 1250 °C. At 1300–1400 °C, only the SiC peak was observed, which indicated the formation of SiC without any residues. Morphological analysis of the SiC synthesised at 1300–1400 °C showed that the particle size increased with the increase in the synthesis temperature. Hence, 1300 °C was considered as a suitable synthesis temperature to synthesise fine SiC powders. To obtain high-purity SiC, the SiC powder was washed with a 5 wt% HF solution several times, which led to a steady decrease in the oxygen content of the powder. After three washing cycles, the oxygen content saturated at 0.11%. Thus, high-purity SiC can be synthesised using poly-Si wafers recovered from waste poly-Si PV cells.

### Acknowledgments

This work was supported by the ‘Human Resources Program in Energy Technology’ of the Korea Institute of Energy Technology Evaluation and Planning (KETEP) and the project for ‘New Business R&D Voucher’ between Industry, Academy, and Research Institute funded by the Korea Ministry of SMEs and Startups in 2019 (Project No. S2718404).

### References

1. W.H. Huang, W.J. Shin, L. Wang, W.C. Sun, and M. Tao, *Sol. Energy*. 144 (2017) 22-31.
2. Y. Xu, J. Li, Q. Tan, A.L. Peters, and C. Yang, *Waste Manag.* 75 (2018) 450-458.
3. Y.S. Zimmermann, C. Niewersch, M. Lenz, Z.Z. Kül, P.F.X. Corvini, and A. Schäffer, *T. Wintgens, Environ. Sci. Technol.* 48[22] (2014) 13412-13418.
4. M. Goe, G. Gaustad, *Sol. Energy Mater. Sol. Cells*. 156 (2016) 27-36.
5. H. Zhang, W. Ding, K. He, and M. Li, *Nanoscale Res. Lett.* 5[8] (2010) 1264-1271.
6. R. Rajarao, R. Ferreira, S.H.F. Sadi, R. Khanna, and V. Sahajwalla, *Mater. Lett.* 120 (2014) 65-68.
7. G.M. Kim, G.S. Cho, D.S. Lim, and S.W. Park, *J. Ceram. Process. Res.* 11[3] (2010) 377-383.
8. B.N. Pushpakaran, A.S. Subburaj, S.B. Bayne, and J. Mookken, *Renew. Sust. Energy Rev.* 55 (2016) 971-989.
9. F. Lomello, G. Bonnefont, Y. Leconte, N. Herlin-Boime, and G. Fantozzi, *J. Eur. Ceram. Soc.* 32 (2012) 633-641.
10. J.H. Kim, C.Y. Kim, and S.C. Choi, *J. Korean Ceram. Soc.* 55[5] (2018) 440-445.
11. G.S. An, J.R. Shin, J.U. Hur, A.H. Oh, B.G. Kim, Y.G. Jung, S.C. Choi, *J. Alloys Compd.* 798 (2019) 360-366.
12. G.S. An, S.W. Choi, D.H. Chae, H.S. Lee, H.J. Kim, Y.J. Kim, Y.G. Jung, and S.C. Choi, *Ceram. Int.* 43 (2017) 12888-12892.
13. G.S. An, D.H. Chae, J.U. Hur, A.H. Oh, H.H. Choi, S.C. Choi, Y.S. Oh, and Y.G. Jung, *Ceram. Int.* 44 (2018) 2-6.
14. G.S. An, J.S. Han, J.R. Shin, D.H. Chae, J.U. Hur, H.Y. Park, Y.G. Jung, and S.C. Choi, *Ceram. Int.* 44 (2018) 12233-12237.
15. R. Wu, C. Zhang, J. Zhao, and Y. Bai, *J. Ceram. Process. Res.* 15 (2014) 433-440.
16. S. Larpkiattaworn, P. Ngerchuklin, W. Khongwong, N. Pankurdee, and S. Wada, *Ceram. Int.* 32 (2006) 899-904.
17. A. Najafi, F.G. Fard, H.R. Rezaie, and N. Ehsani, *Powder Technol.* 219 (2012) 202-210.
18. J. Ma, G.Y. Li, Z.Y. Chu, X.D. Li, Y.H. Li, and T.J. Hu, *Carbon*. 69 (2014) 634-637.
19. K. Xiang, X. Wang, M. Chen, Y. Shen, H. Shu, and X. Yang, *J. Alloys. Compd.* 695 (2017) 100-105.